



Nano Scale Disruptive Silicon-Plasmonic Platform for Chip-to-Chip Interconnection

D 6.3 – Report on chip to chip interconnect characterization

Deliverable no.: D6.3
Due date: 31/07/2014
Actual Submission date: 22/09/2014
Authors: ETHZ
Work package(s): WP6
Distribution level: RE¹ (NAVOLCHI Consortium)
Nature: document, available online in the restricted area of the NAVOLCHI webpage

List of Partners concerned

Partner number	Partner name	Partner short name	Country	Date enter project	Date exit project
1	Karlsruher Institut für Technologie	KIT	Germany	M1	M36
2	INTERUNIVERSITAIR MICRO-ELECTRONICA CENTRUM VZW	IMEC	Belgium	M1	M36
3	TECHNISCHE UNIVERSITEIT EINDHOVEN	TU/e	Netherlands	M1	M36
4	RESEARCH AND EDUCATION LABORATORY IN INFORMATION TECHNOLOGIES	AIT	Greece	M1	M36
5	UNIVERSITAT DE VALENCIA	UVEG	Spain	M1	M36
6	STMICROELECTRONICS SRL	ST	Italy	M1	M36
7	UNIVERSITEIT GENT	UGent	Belgium	M1	M36

¹ **PU** = Public
PP = Restricted to other programme participants (including the Commission Services)
RE = Restricted to a group specified by the consortium (including the Commission Services)
CO = Confidential, only for members of the consortium (including the Commission Services)

Deliverable Responsible

Organization: ETH Zurich
Contact Person: Claudia Hoessbacher
Address: Institute of Electromagnetic Fields (IEF)
ETZ K 93
Gloriastrasse 35
Switzerland
Phone: +41 44 632 67 68
E-mail: choessbacher@ethz.ch

Executive Summary

This report contains the implementation and characterization of a prototype of the plasmonic interconnect, built by integrating an array of the plasmonic Mach-Zehnder modulators described in the previous reports, in particular D6.1. A transmitter operating at 4×36 Gbit/s is shown on a footprint that is only limited by the size of the high-speed contact pads. The array is contacted through a multicore fiber with a channel spacing of $50 \mu\text{m}$ (D6.2).

Change Records

Version	Date	Changes	Author
1 (submission)	2015-09-22		Claudia Hoessbacher

Plasmonic MZM array

As a first step towards NAVOLCHI's system demonstrator, we have fabricated an array of four plasmonic Mach-Zehnder modulators (MZMs). A multicore fiber (MCF) with a 50 μm channel spacing connects the array. The transmitter is demonstrated to operate at 4×36 Gbit/s. The array has been characterized for optical interchannel crosstalk which was found to be below -31 dB. No electrical crosstalk was observed. The MZMs showed no bandwidth limitation up to 70 GHz. The individual MZMs comprise plasmonic phase modulator sections that are as short as 12.5 μm . This allows for a dense arrangement of the MZMs that is only limited by the size of the contact pads needed for addressing the devices with electrical probes. The devices are able to operate over a broad spectral range of >100 nm.

Design and fabrication

A microscope image of the MZM array is depicted in Fig. 1. The key elements are 12.5 μm long PPMs. They are formed by two gold (Au) electrodes separated by a 75 nm wide slot. For direct electrical probing with standard 100 μm pitched ground-signal-ground (GSG) probes we increased the distance between MZMs to 300 μm . However, the actual footprint required by the devices is only a few tens of μm^2 . This leaves ample room for scaling down once electronics and photonics are cointegrated. The optical interface consists of GCs with a 50 μm spacing and is matched to the channel spacing of the multicore fiber (MCF).

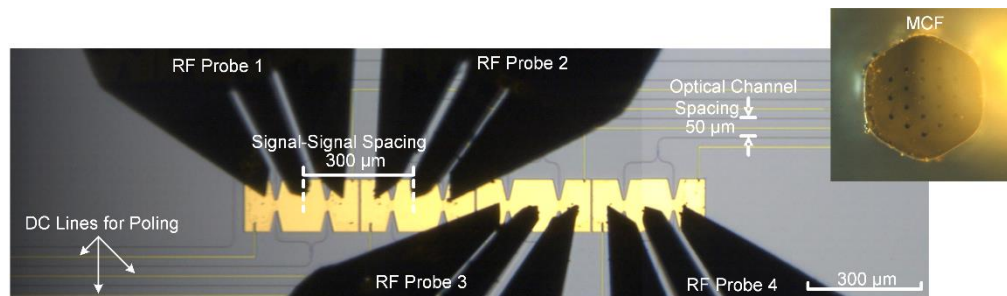


Fig. 1 Optical microscope image of the fabricated four-channel MZM array contacted by RF probes. The plasmonic phase modulators are 12.5 μm long with slot widths of 75 nm.

The MZM array was produced in-house on a silicon-on-insulator (SOI) wafer. E-beam lithography in combination with dry-etching was applied to pattern the photonic components, namely the Si waveguides ($h_{\text{Si}} = 220$ nm, $w = 450$ nm), MMIs and GCs. A silicon oxide cladding was applied and structured by dry and wet etching prior to the fabrication of the PPMs. The PPMs were realized with a lift-off process applied to e-beam evaporated gold ($h_{\text{Au}} = 150$ nm). In a last step the nonlinear optical material DLD164 ($r_{33} \approx 180$ pm/V) was applied by spin-coating and poled by applying a DC electric field at the glass transition temperature of the material. Simultaneous electric field poling of several modulators at the same time is not straight forward. Single devices cannot be poled one after another. Due to heating of the chip during the poling process, electro-optic molecules in previously poled devices would relax back into a randomized order, thus the devices would lose their poling. Lattice hardening (crosslinking) of the ordered molecules is a solution for this problem, but the material used in the presented experiments does not offer this feature. Therefore, all devices of the array have to be poled at the same time. One possibility is to contact all four MZMs individually. However, contacting eight DC probes within a few hundreds of μm is rather impractical. We therefore investigated two schemes to pole multiple devices at the same time while using only two DC probes, see Fig. 2.

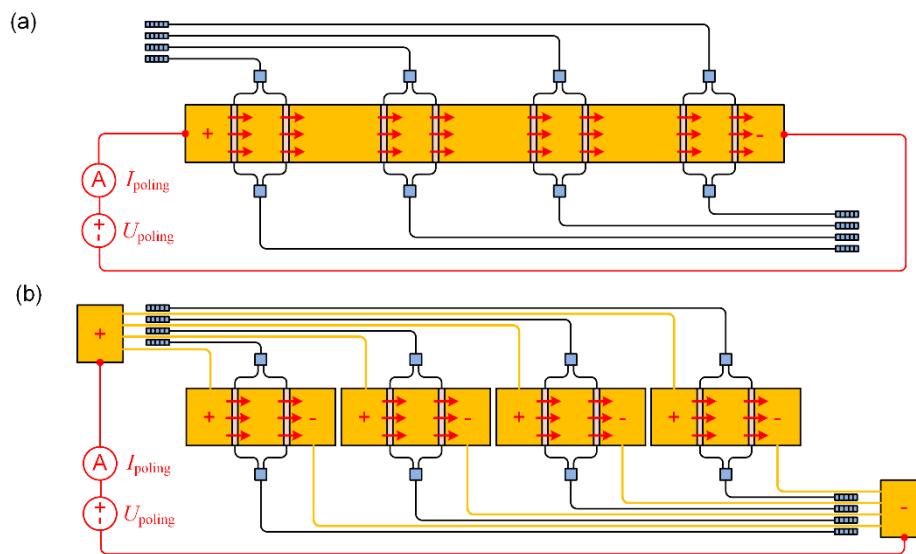


Fig. 2 Possible poling schemes. (a) Serial poling: The outer electrodes of the individual MZMs are connected, while the two most outer electrodes are contacted using DC probes to apply the poling field. The required voltage is the sum of the voltages across each component. (b) Parallel poling: The two outer electrodes of the individual MZMs are connected to poling electrodes. The voltage applied to the poling electrodes and the voltage across each component are the same and lower than for the serial scheme.

Connecting the outer electrodes of the individual modulators in series allows a serial poling, see Fig. 2(a). However, there are two major disadvantages of this scheme: First, the poling voltage required for an array of n devices is n times higher than for a single device. This can result in high voltages making special requirements for voltage source and safety precautions mandatory. Second, in case of dielectric breakdown or electrical short in one single modulator arm, the voltage across the other devices will increase significantly. This can lead to a cascade effect that destroys all modulators being poled. An alternative approach is parallel poling of the devices as illustrated in Fig. 2(b). In this scheme, the voltage applied to the poling electrodes and to each modulator is the same. Therefore, the required poling voltage is not higher than for single device poling. In case of dielectric breakdown or a short in one device, the voltage at the other modulators will not increase. The damaged device would effectively act as an electrical fuse, being destroyed completely by the high current that suddenly flows. After this process, it would appear as an open circuit, while the voltage across the other modulators would stay the same. The remaining modulators would still be poled. The disadvantage of the parallel poling scheme however is, that it requires additional electrical DC lines to connect the individual electrodes, which is only an additional design effort but does not pose a technical disadvantage. In more complex structures metal/waveguide crossings can be realized by a multiple layer process. This would allow for even easier layouts by introducing a poling layer connected to the modulators by vias. This would allow for parallel poling of all devices on a chip at the same time. Given the advantages of the lower poling voltages our decision was made in favor of the parallel poling scheme, Fig. 2(b).

Characterization

The static characteristics of the array were studied first. The optical extinction ratios of the imbalanced interferometers were found to be in the range of 7.3...23.9 dB with insertion losses

of (12.6 ± 0.7) dB. The plasmonic propagation losses within the active section were ~ 0.9 dB/ μm at a wavelength of 1550 nm. This is higher than the losses of ~ 0.5 dB/ μm as in our previous batch.

To measure the modulation bandwidth of the individual modulators a -3 dBm small signal RF field between 15 GHz and 70 GHz was applied to the devices. The ratio between optical carrier and modulation sidebands was measured with an optical spectrum analyzer (OSA) and normalized to 15 GHz, Fig. 3(a). This technique allows to measure up to highest speeds and is only limited by the maximum frequency of the RF source (70 GHz in this case). However, the spectral resolution caused by the optical filter shape of the OSA limits the measurement to frequencies >15 GHz. Fig. 3(b) depicts the normalized modulation bandwidth of all four channels. The electrical frequency response of the four channels shows no bandwidth limitation up to 70 GHz.

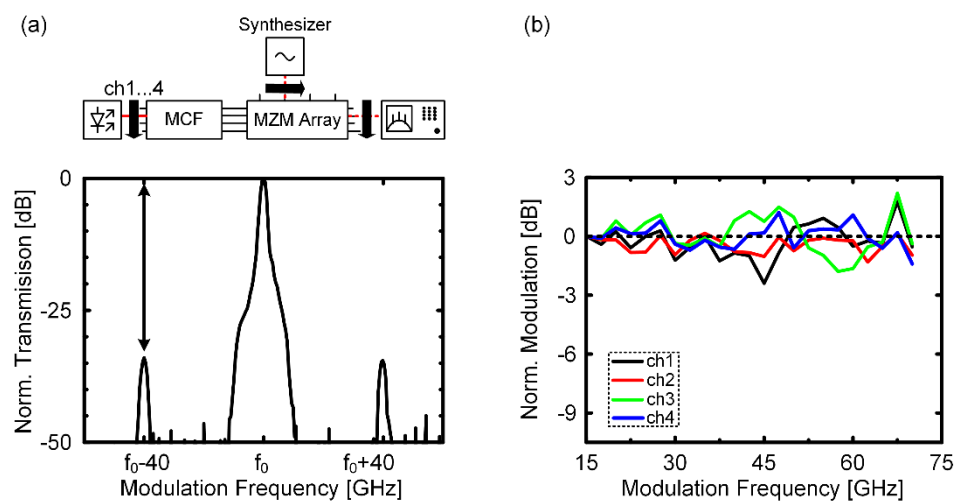


Fig. 3 RF-bandwidth characterization of the MZM array. (a) Experimental setup and measurement technique. The modulators are characterized sequentially using a sinusoidal RF waveform. The ratio of the carrier to the first modulation sideband is measured in the optical spectrum for RF-frequencies between 15 and 70 GHz (here 40 GHz). (b) Normalized modulation frequency response of all channels. The 3 dB bandwidth is above 70 GHz, thus no bandwidth limitation is expected.

To investigate the optical crosstalk of the dense optical interface we fed 4 different wavelengths (1543.5 nm...1545.0 nm) through 4 different channels (ch1...ch4) of the MCF, while coupling to silicon waveguides (WGs) without MZMs. The optical output spectrum of each channel was recorded using an OSA, Fig. 4(a). Crosstalks were found to be lower than -31 dB in any instance. As an example we discuss the crosstalk into channel 2. The spectrum of channel 2 is shown in red. A main peak at 1544.0 nm is found which corresponds to the wavelength fed to channel 2. Besides, smaller peaks at the wavelengths of the neighboring channels appear in the spectrum. The electrical crosstalk between the MZMs was investigated by applying a sinusoidal RF signal to one channel while checking for signs of modulation in the optical signals of the neighboring channels, Fig. 4(b). No modulation sidebands could be observed in a neighbor channel when any of the MZM were modulated. If there should be any crosstalk, it must be -30 dB or less, as can be inferred from the noise level of the OSA with which the measurements were performed.

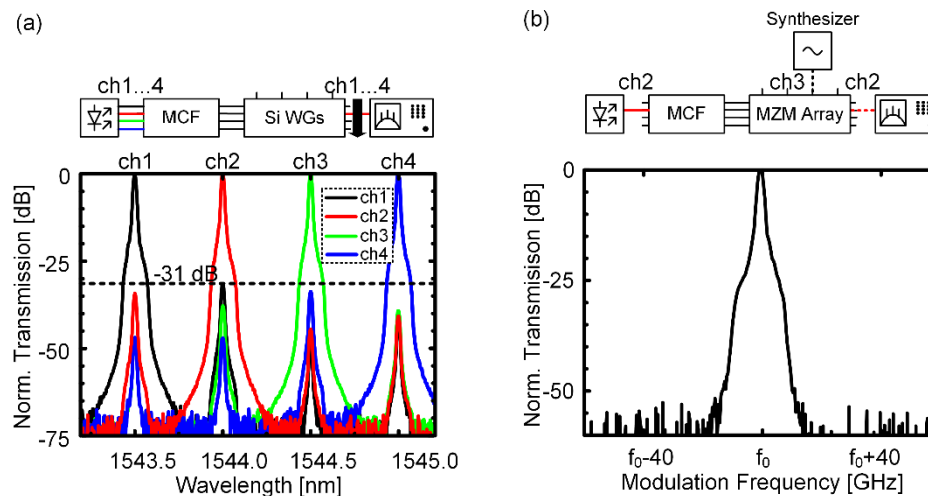


Fig. 4 Optical and electrical crosstalk characterization. (a) Optical crosstalk: Measurement setup for optical crosstalk to channel 2 and recorded optical spectrum of all channels. An optical interchannel crosstalk below -31 dB was found for all channels. The spectra were obtained by coupling four different wavelengths to the MCF. (b) Electrical crosstalk: Measurement setup for electrical crosstalk between channel 3 and channel 2 and recorded spectrum of channel 2 as an example. A sinusoidal RF signal was applied to a certain channel while checking for modulation signs of an unmodulated neighboring channel. An electrical crosstalk below -30 dB was found.

The applicability of plasmonic MZMs in communication systems was verified by data modulation experiments. Data signals with binary phase shift keying (BPSK) at 36 Gbit/s were generated. The experimental setup is depicted in Fig. 5. Four CW laser sources (1549.3 nm to 1552.7 nm, $\Delta\lambda \approx 1$ nm) were coupled to the array via the MCF. Two digital-to-analog converters (72 GSa/s, 6 bit) generated uncorrelated, differential signals D_1 and D_2 (pulse shape: square-root-raised cosine, roll off $\alpha = 1$) with De Bruijn bit sequences (DBBS 2^{15}) that were amplified to 4 V_{pp} by RF amplifiers. $D_1, D_2, \bar{D}_1,$ and \bar{D}_2 were fed to the single ended modulators by two GSGGSG probe-arrays. The four channels were received sequentially with a standard single mode fiber in a coherent receiver. Pre-distortion and post-equalization of the electrical signal was used to mitigate the frequency dependence of the RF amplifiers and the DACs. Fig. 6 depicts the measured optical eye diagrams and constellation diagrams for all four channels at 36 Gbit/s. All channels have bit error ratios (BERs) below the FEC limit of 2×10^{-3} (7 % overhead); no error was detected within the 20 million recorded bits for channel 3.

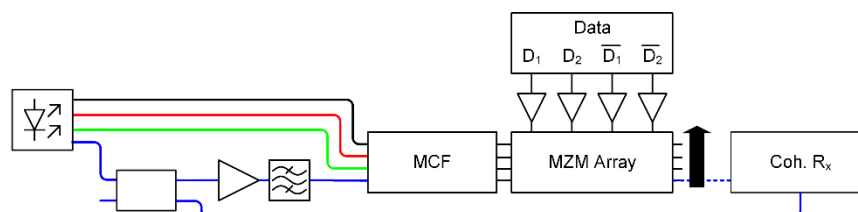


Fig. 5 Experimental setup for data modulation experiments. Four lasers with different wavelengths ($\Delta\lambda \approx 1$ nm at $\lambda \approx 1550$ nm) were coupled to a multicore fiber (MCF) and the modulator array. Four electrical data streams were fed to the modulators by two independent DACs. The laser of the channel under test was amplified before coupling to the MCF. The modulated light of the channel under test was received by a coherent receiver. The laser source of the channel under test was also used as local oscillator in the receiver.

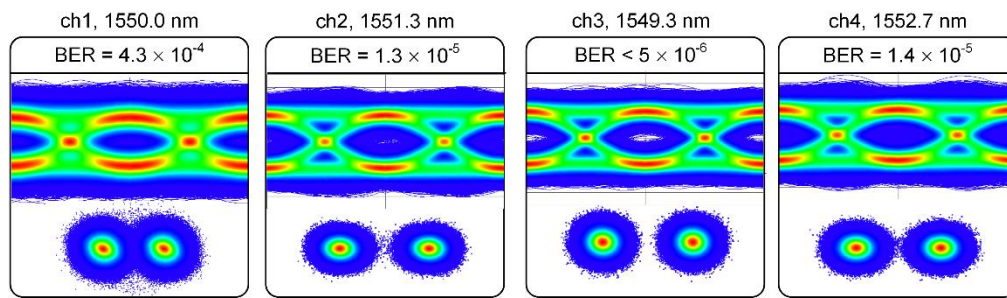


Fig. 6 Optical eye and constellation diagrams with bit error ratios (BER) of the data experiments (BPSK) at data rates of 36 Gbit/s. All four channels have a BER below the FEC limit of 2×10^{-3} .